Collisional-radiative model for heliumlike ions: Application to intermediate-density plasmas

Takashi Fujimoto
Department of Engineering Science, Kyoto University, Kyoto 606, Japan

Takako Kato
Institute of Plasma Physics, Nagoya University, Nagoya 464, Japan
(Received 17 January 1984)

In order to interpret the spectral-line intensities emitted from various plasmas, a collisional-radiative-model program has been constructed for heliumlike ions. In this model a population of 61 excited levels is considered, and excitation, deexcitation, ionization and three-body recombination by electron collisions, spontaneous transition, radiative recombination, and dielectronic recombination have been included. For these processes, the most reliable rate coefficients, experimental or theoretical, have been employed. A detailed account is given of the program along with the review of the rate coefficients adopted. As an example of its applications, line-intensity data for theta-pinch plasmas are analyzed; for oxygen the three sets of experiments are consistent with the present calculation. For the case of carbon, however, the intensity ratio cannot be interpreted consistently on the assumption of the ionizing-plasma model. Rather, it is strongly suggested that the plasma has a significant contribution from the recombining-plasma component.

I. INTRODUCTION

The intensity of atomic and ionic lines emitted from a plasma is determined by the state of the plasma (e.g., its electron density n_e and temperature T_e) as well as by the atomic parameters of transitions that are related to, directly or indirectly, the intensity of the emission lines concerned (e.g., transition probability, and excitation and ionization cross sections). In plasma spectroscopy experiments the observed line intensity is interpreted by using a model which incorporates the former quantities with the latter. For instance, by knowing or assuming n_e and T_e of the plasma, we sometimes employ the corona model to interpret the emission-line intensity by using appropriate atomic parameters. In general, however, we may adopt other models, e.g., the capture-cascade model for the same plasma, and the same experimental data may be analyzed in terms of this. Then we would have a completely different result[1] for the characteristics of the plasma. Therefore, in order to obtain a correct understanding of the plasma under study, it is essential to employ a model that describes the plasma correctly as well as to adopt reliable atomic parameters for the important transitions.

Among the models which describe the ionization and recombination of atoms and ions, and excited-level populations in a plasma the most general and complete is the collisional-radiative model;[2] this model includes the corona, capture-cascade models, and LTE (local thermodynamic equilibrium) as its limiting cases.[1,3]

The present authors have constructed a computer code of the collisional-radiative model for heliumlike ions, and it has been applied to the solar corona plasma[4] and to the laser-produced aluminum plasma.[5] In the former case the calculated line-intensity ratio was compared with the observation and the magnitude of the excitation cross section was assessed. In the latter the observed emission-line intensities determined the plasma state, i.e., the plasma was in the recombining phase. In both cases, however, the plasma was of very low density or of very high density, and the dominant features of the populations of the levels were found to be described by simple models: the corona model in the former case and LTE in the latter.

In the present paper, we apply the collisional-radiative model to intermediate-density plasmas. In these plasmas collisional transitions from excited levels, for instance, are important. Under these conditions the simple corona model is obviously inadequate, and even the modified corona model may not be sufficient for a quantitative analysis of the experimental data. Only the collisional-radiative model describes these plasmas, and by applying this we can extract from the experimental data reliable information on atomic parameters, e.g., excitation cross section.

In the next two sections, a detailed account is given of the collisional-radiative model code. In the last section several experimental results on the theta-pinch plasma are analyzed by our model, and a strong doubt is raised on the state of the plasma for which the intensity measurement has been reported.

II. ATOMIC PARAMETERS

In this section a brief account is given of the atomic parameters employed in our computer code. Further details and numerical values are presented elsewhere.[6]

A. Energy levels

All the levels ($1snl\ ^{1,3}L$) having a principal quantum number $n \leq 7$ are treated separately, except for the levels

having the orbital angular momentum $L > 3$. These latter levels with the same n are grouped together to form a single level. The level $1s2p\,^3P$ is resolved into the three fine-structure components $^3P_{0,1,2}$. For the levels $8 < n < 10$, all of the $S,P,D,\ldots$ levels are grouped together. The levels with $n \geq 11$ are approximated by the hydrogenic levels having statistical weights twice those of hydrogenic ions. In the calculation, the upper limit of the levels considered is $n=20$; the total number of levels whose population density is calculated is 61. The levels with $21 < n < 24$ are assumed to be in LTE.

Term values of several low-lying levels for small nuclear charge z, are given in Refs. 7 and 8. It has been found that these term values T cm^{-1} as functions of z are well fitted to

$$\sqrt{T} = (1+a)\sqrt{R_\infty}(z-1-b)/n \ , \tag{1}$$

where R_∞ is the Rydberg constant. In Eq. (1) the parameter a, which is of the order of 10^{-3}, represents the deviation from the Mosely law. The parameter b corresponds to the quantum defect. For the levels of $n=2$, a and b are determined from Refs. 7 and 8. For other levels a is put equal to 0 and b is set proportional to $1/z$ starting from the quantum defect of neutral helium levels $z=2$.

Owing to the spin-orbit interaction, the wave function of a state, e.g., 2^3P_1, becomes a mixture of pure singlet (2^1P_1), and pure triplet (2^3P_1) wave functions of a common J. The amount of this admixture is conveniently expressed by a mixing coefficient. Reference 9 gives these coefficients. For all of the levels this mixing is taken into account: the atomic parameters for transitions between those levels, i.e., transition probability and excitation, and deexcitation rate coefficients, are redistributed between these mixture states.

B. Transition probabilities

For important transitions between low-lying levels theoretical and experimental data are available; for optically allowed transitions Ref. 10 gives theoretical data, and for optically forbidden transitions theoretical[10–12] and experimental[13,14] transition probabilities are available. These values as functions of z are fitted to approximate expressions

$$A = \sum_{n=1}^{2} A_n (z - x_n)^{y_n} \ , \tag{2}$$

where A_n, x_n, and y_n are adjustable parameters. The approximation (2) is accurate to within 10% as shown in Fig. 1, as an example.

For other optically allowed transitions oscillator strengths are fitted by the formula

$$f = f_H - \Delta f / z \tag{3}$$

where f_H is the hydrogenic oscillator strength[15] for the corresponding optically allowed transitions. Equation (3) is employed for transitions with $\Delta n \neq 0$ and for $\Delta n = 0$; in the latter case $f_H = 0$ and $\Delta f < 0$. For transitions between high-lying levels, Δf is determined from the oscillator strength for $z=2$ (neutral helium).[16,17] Figure 2 gives a few examples.

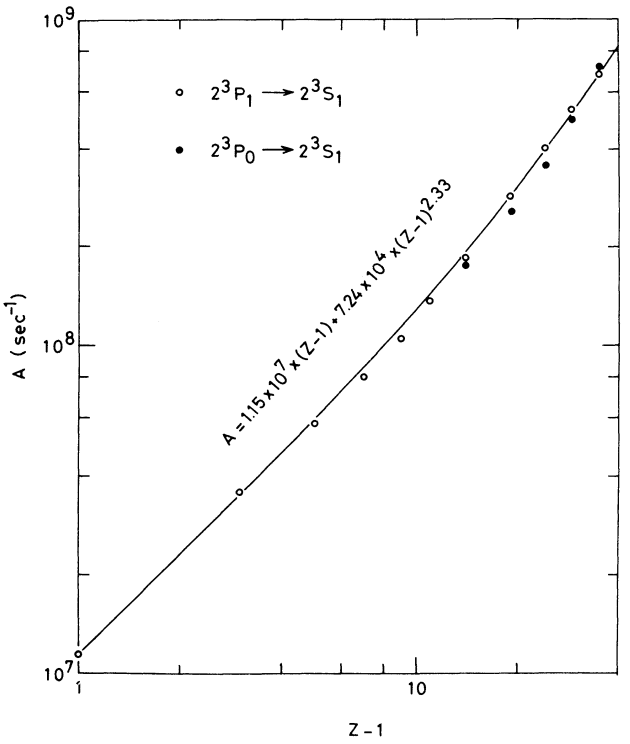

FIG. 1. Theoretical transition probabilities (Ref. 10) and the approximation (solid line) as a function of z.

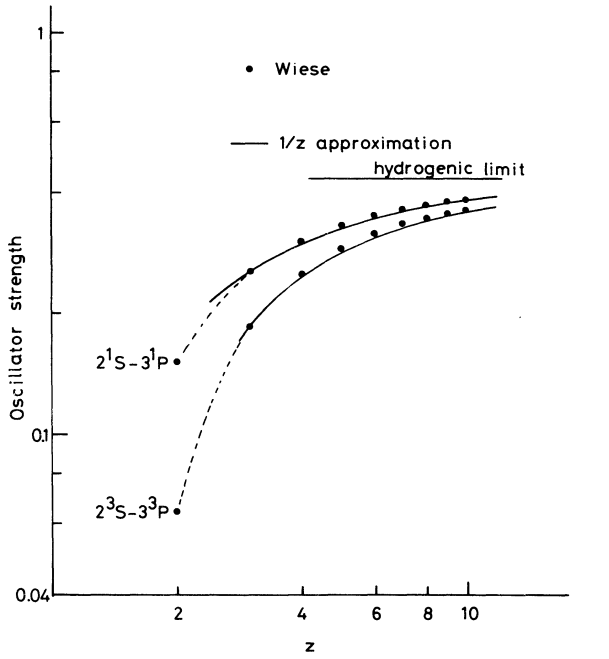

FIG. 2. Theoretical (Ref. 16) and approximate values (solid line) of oscillator strength as a function of z.

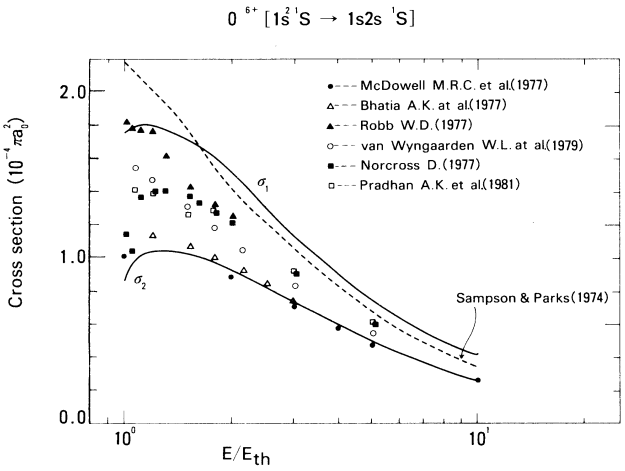

FIG. 3. Excitation cross sections for 1^1S-2^1S of O VII. σ_1 and σ_2 indicate the upper and the lower bounds, respectively. Several theoretical values (Refs. 18—24) are shown.

C. Excitation cross section

There are numerous calculations of the cross sections from the ground level to low-lying excited levels. Agreement between them, however, is not always satisfactory. The only exception is the cross section for 1^1S-2^3P. All of the existing calculations,[18—23] agree within 10% (except for the resonance structure presented in Ref. 24). In our previous study[4] we relied on the averaged cross section for this transition and tried to assess the magnitude of other cross sections relative to this cross section. We concluded that for 1^1S-2^1P the distorted wave calculations[19,20,22] appeared to give the most reasonable cross section. We found that our rate coefficient is smaller than that given in Ref. 24 typically by 8% for 1^1S-2^3P and larger by 2% for 1^1S-2^1P for the temperature range of practical interest. In Ref. 4 we could not assess the cross section for 1^1S-2^3S.

In this paper, for the cross section 1^1S-2^3S, we adopt the analytic formula that gives the rate coefficient in agreement with that of Ref. 24. For 1^1S-2^1S existing calculations[18—24] are summarized in Fig. 3, and we discuss this cross section later. For other transitions we rely primarily on the infinite-z hydrogenic approximation by Sampson and Parks;[18] for the optically allowed transitions the original cross section is scaled on the basis of the oscillator strength as given in Sec. B so as to give the correct Bethe limit. Our rate coefficients for the transitions between the excited levels are in good agreement with Ref. 24, except for some of the transitions between singlet-triplet levels. For these transitions our value is smaller by a factor of 2. We suppose this discrepancy is due to our neglect of the resonance structure. In order to take this into account we have multiplied our original rate coefficient by 2, although these transitions do not play a significant role in any case.

D. Ionization cross sections

Ionization cross sections from the lowest-lying levels are given in Ref. 25. These are well fitted by the semi-

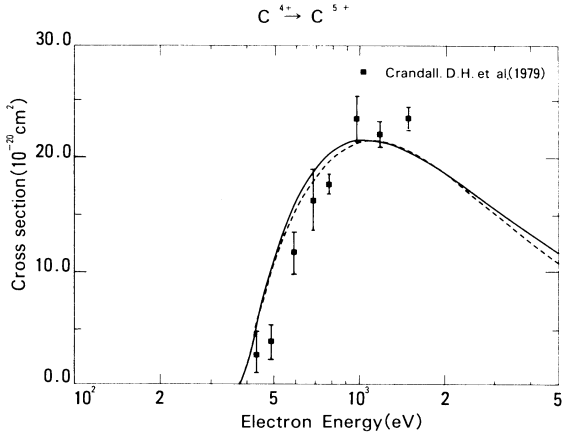

FIG. 4. Ionization cross section for C V by Ref. 25 (dotted line) and Ref. 26 (solid line). Experiment is Ref. 28.

empirical formula of Ref. 26. Reference 27 compares the cross sections given by Ref. 26 with the available experimental results for the ionization from the ground state, and it is found that the formula of Ref. 26 fits the experiment well. Therefore, the ionization cross sections from all of the levels are approximated by the above semiempirical formula of Ref. 26. Figure 4 gives an example of the comparison of empirical formulas with the experiment.[28]

E. Photoionization cross sections

Reference 29 shows that the photoionization cross section from the ground level is well represented by the hydrogenic cross section multiplied by 2. For other levels the hydrogenic approximation should be valid since even for neutral helium n^1P and n^3P levels ($2 \leq n \leq 5$) the hydrogenic approximation is fairly good.[30,31] Therefore, for all of the levels cross sections are approximated by the hy-

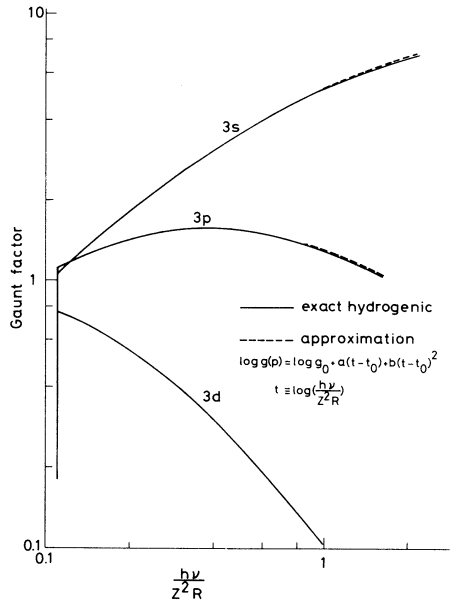

FIG. 5. Gaunt factor for photoionization from $n=3$ levels. Solid and dotted lines indicate the exact hydrogenic results and the approximate ones, respectively.

drogenic ones. The latter cross sections[32] or the Gaunt factors[15] may well be approximated by

$$\ln g(\nu)=\ln g_0+c(t-t_0)+d(t-t_0)^2 \tag{4}$$

with

$$t=\ln(h\nu/R_\infty) \tag{5}$$

where c and d are fitting parameters and ν is the frequency of the ionizing photon. Figure 5 shows an example of the Gaunt factor for photoionization from $3l$ levels.

The excitation, ionization, and photoionization cross sections given above are integrated over a Maxwellian distribution of electron velocities to give respective rate coefficients: i.e., excitation and deexcitation, ionization and three-body recombination, and radiative recombination rate coefficients.

F. Dielectronic recombination

Recombination accompanying the stabilizing transition $2pnl$-$1snl$ following the dielectronic capture is included. For the doubly excited levels $(2pnl)\,^{2S+1}L_J$ with $n\geq 3$, the autoionization probability is calculated from the direct and exchange reactance matrix elements[33] for the excitation cross section of hydrogenic $1s$-$2p$, and the stabilizing transition probability is given by the spontaneous transition probability of hydrogenic $2p$-$1s$. For the levels $(2p2l)\,^{2S+1}L_J$, the autoionization and stabilizing transition probabilities are estimated from Ref. 34. Dielectronic recombination rate coefficients are readily obtained on the basis of the LS-coupling scheme. Figure 6 shows an example of dielectronic recombination rate coefficients to various levels.

III. COLLISIONAL-RADIATIVE MODEL

According to the method of the quasi-steady-state solution or the collisional-radiative model, ionization and recombination of the heliumlike ions in a plasma is described by

$$\begin{aligned}\dot{n}(1)&=-\dot{n}_{\rm H}\\&=-S_{\rm CR}n(1)n_e+\alpha_{\rm CR}n_{\rm H}n_e\ ,\end{aligned} \tag{6}$$

where $n(1)$ and $n_{\rm H}$ are the densities of the ground state of heliumlike and hydrogenic ions, respectively. The effective rate coefficients $S_{\rm CR}$ and $\alpha_{\rm CR}$ are called the collisional-radiative ionization and recombination rate coefficients, respectively, and they are functions of n_e and T_e of the plasma.

The population density of an excited level p of the heliumlike ion is given as a superposition of the two components; i.e., the contribution connected to the hydrogenic ions and that to the ground level of heliumlike ions;

$$\begin{aligned}n(p)&=n_0(P)+n_1(p)\\&=Z(p)r_0(p)n_{\rm H}n_e+[Z(p)/Z(1)]r_1(p)n(1)\end{aligned} \tag{7}$$

with

$$Z(p)=g(p)(h^2/2\pi mkT_e)^{3/2}\exp[\chi(p)/kT_e]/2g_{\rm H}\ .$$

Here $g(p)$ and $\chi(p)$ are the statistical weight and the ionizational potential of level p, respectively, $g_{\rm H}=2$ is the statistical weight of the ground-state hydrogenic ion and $r_0(p)$ and $r_1(p)$ are called the population coefficients, which are functions of n_e and T_e. Other symbols are used in the usual meanings.

By using the rate coefficients and the transition probabilities as described in the preceding section, these coefficients $S_{\rm CR}$, $\alpha_{\rm CR}$, $r_0(p)$, and $r_1(p)$ are calculated for various conditions of T_e and n_e.

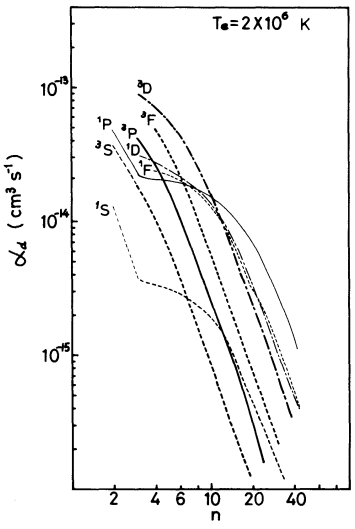

FIG. 6. Dielectronic recombination rate coefficient into various levels of B IV. $T_e=2\times10^6$ K.

IV. COMPARISON WITH EXPERIMENT

In our previous paper[4] we have compared the results of our calculation with the observation of the prominent lines emitted from the solar corona plasma in order to test our computer program as well as to assess the excitation cross sections adopted in it. Our program has also been successfully applied to the analysis of the laser-produced aluminum plasma.[5] The plasmas treated in these papers, however, are either of very low density or of very high density; in the former plasma the corona model or the capture-cascade model may be valid, and in the latter plasma, LTE or the ladderlike mechanism should be the dominant characteristics of the excited level populations.[1] In both these cases the population density distribution is relatively insensitive to the magnitude of the individual transition rates (except for those pertinent to the ground level in the corona model). Thus the agreement of the calculation with the observation does not necessarily indicate the correctness of individual rate coefficients (except for, of course, the excitation rate coefficients from the ground level) nor of the computer program. In this section the line-intensity ratio obtained from theta-pinch plasmas is analyzed; for these plasmas electron density is relatively high, and therefore atomic parameters pertinent to excited levels, e.g., excitation cross section from the metastable levels, become essential in determining the population densities of the line-emitting levels.

We start with the assumption that the plasmas for which the line intensities have been observed are in the ionizing phase,[1] or $n_H/n(1)$, the ratio of the hydrogenic ion density to the heliumlike ion density, is much smaller than that given under the ionization equilibrium condition S_{CR}/α_{CR}.

First, we take the experiments on oxygen. Figure 7 shows the intensity ratio $R/(R+I)$, where R stands for the resonance-line (1^1S-2^1P) intensity and I is the intercombination-line (1^1S-2^3P) intensity. Experimental value is given by three groups.[35–37] The number associated with each of the data points represents the electron temperature as given in the original papers. Under these conditions 2^3S and $2^3P_{0,2}$ populations are almost completely equilibrated each other, but the resonance and the intercombination lines are so strong for 2^1P and 2^3P_1, respectively, that their populations are not in equilibrium with $2^{1,3}S$ level populations. In Fig. 7 the theoretical calculation is also shown. For the cross section of 1^1S-2^1S in Fig. 3 we pose the upper bound σ_1 and the lower bound σ_2 for the existing calculations. The results of the calculation corresponding to these two cases are shown in Fig. 7 for two temperatures $T_e=200$ and 300 eV. For $n_e<10^{16}$ cm^{-3}, the gradual increase in the ratio corresponds to the increase in the 2^1P population due to the stepwise excitation via 2^1S and to the gradual decrease in the 2^3P level populations due to the depletion by ionization from this level.

First, we look at the data by Pospieszczyk;[37] the ratio is roughly consistent with the calculation, but its temperature dependence is contrary to that expected from the calculation: The ratio should increase with an increase in the temperature owing to the difference in the energy dependence of the excitation cross section of 1^1S-2^3P and of

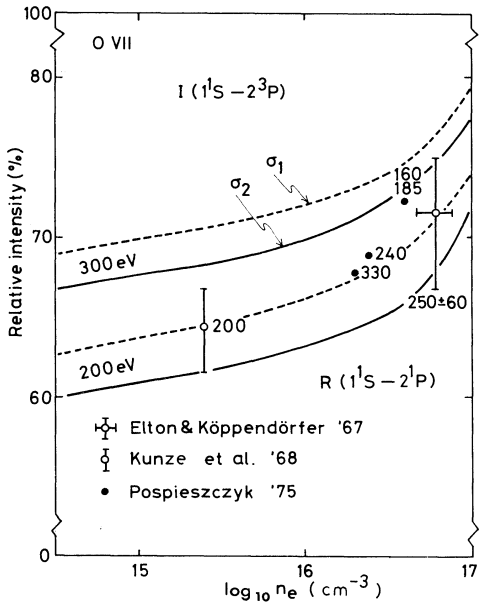

FIG. 7. Intensity ratio $R/(R+I)$ for O VII, where R is the intensity of the resonance line and I is that of the intercombination line. Dotted line and solid line are the calculated results using the cross section of upper bound σ_1 and lower bound σ_2 in Fig. 3, respectively.

1^1S-2^1P. We suppose that his temperature determination based on the absorption method has given an erroneous result. Therefore, we put his data out of our further consideration.

The data by Kunze *et al.*[36] favors the upper bound σ_1 for the excitation cross section 1^1S-2^1S, while that by Elton and Köppendörfer[35] favors the lower bound σ_2. However, if we take into account the experimental uncertainty, both the data are consistent with either of the cross sections σ_1 and σ_2. This ambiguity comes partly from the fact that the contribution from the excitation 1^1S-2^1S to the intensity R is small, i.e., it is 17% for σ_1 or 15% for σ_2 ($T_e=250$ eV, $n_e=6.2\times10^{16}$ cm^{-3}, corresponding to Ref. 35).

Under the above condition of Elton and Köppendörfer, our calculation gives the following rate coefficients: for 1^1S-2^1S, 2.9×10^{-12} cm^{3}s^{-1} (σ_2 has been assumed); for 1^1S-2^1P, 16.0×10^{-12}; for 1^1S-2^3S, 1.4×10^{-12}; for 1^1S-2^3P, 7.3×10^{-12}. These are compared with the original conclusion of 31×10^{-12} cm^{3}s^{-1} for 1^1S-(2^1S+2^1P) and 15×10^{-12} cm^{3}s^{-1} for 1^1S-(2^3S+2^3P). The absolute magnitude of their rate coefficients was determined from the observed absolute intensity of the lines 2^3S-2^3P of 90 ± 40 W cm^{-3} and estimated density of $n(1^1S)$ of O^{6+} ion of $(1.9\pm0.6)\times10^{14}$ cm^{-3}. Our calculation gives the absolute intensity of (71 ± 22) W cm^{-3} which is consistent with the observation. Therefore, the factor-of-2 difference in the excitation rate coefficients between the original and present results is interpreted as partly due to the assumption of equilibrium of the $2S$ and $2P$ populations and to the neglect of the cascading contribution in the original paper and partly due to the different rate coefficients for ionization from the 2^3S and 2^3P levels.

In the high-density region $n_e>10^{16}$ cm^{-3} with an increase in n_e the net depopulation from the 2^3P level makes the relative population density of this level decrease resulting in a steep increase in the ratio. It is found that the ionization and the singlet-triplet excitation transfer constitute the dominant part of the net collisional depopulation from 2^3P. We could determine the rate coefficient for the net depopulation by using the point by Elton and Köppendörfer. However, the uncertainty in their density determination makes it difficult. Experimental data for still higher density should give information on the ionization rate coefficient. This point will be discussed later in discussing the experiment on carbon.

Among the fine-structure levels $2^3P_{0,1,2}$, $J=1$ level has a large transition probability to 1^1S, and its population is lower than others. The collisional depopulation process, predominantly deexcitation to 2^3S, makes this population unbalance decrease. This feature does not depend on whether the plasma is ionizing or recombining. Engelhardt *et al.*[38] have measured the intensity ratio of the fine-structure components of 2^3S-$2^3P_{0,1,2}$ transitions. Figure 8 reproduces their result. The result of our calculation is also shown, and it is in good agreement with the experiment. Our total depopulation rate coefficient from the 2^3P level ($2^3P_{0,1,2}$ levels are assumed to have equal collisional rate coefficients) is 1.12×10^{-8} cm^{3}s^{-1}. The detail is, for 2^3P-2^3S, 8.0×10^{-9} cm^{3}s^{-1}; for 2^3P-3^3D, 1.7×10^{-9}, 2^3P-ion, 0.3×10^{-9}. If our total depopulation

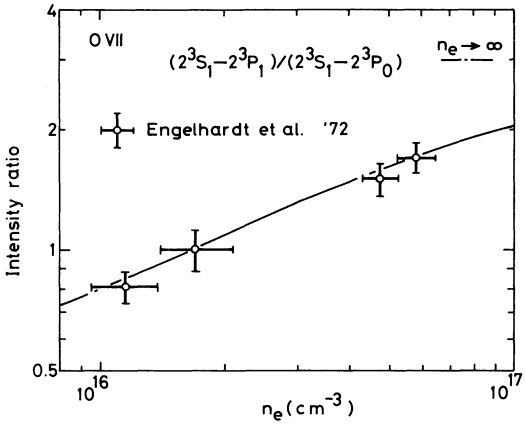

FIG. 8. Intensity ratio of the fine-structure component of $I(2^3S_1\text{-}2^3P_1)/I(2^3S_1\text{-}2^3P_0)$ (Ref. 38). The solid line shows our calculated results. $T_e=215$ eV.

rate coefficient were reduced by 10% we would have better agreement with the experiment. This is compared with the original conclusion of 1.05×10^{-8} cm^3 s^{-1}.

Next, we examine the experiment for carbon. As suggested earlier, the critical electron density at which the net collisional depopulation rate and radiative decay from the 2^3P level become comparable in magnitude is smaller for carbon than for oxygen; it is about 5×10^{15} cm^{-3}. Kunze *et al.*[36] assume that the dominant part of the depopulation is the singlet-triplet excitation transfer, and they give the excitation transfer rate coefficient of 1.1×10^{-9} cm^3 s^{-1} for C^{4+}. In our calculation, however, the corresponding rate coefficient is about 1×10^{-10} cm^3 s^{-1} while the ionization rate coefficients is 1.6×10^{-9} cm^3 s^{-1}. Thus, the latter process is responsible for the steep increase in the ratio. At about this density it is expected that the intensity ratio I/R is sensitive to the ionization rate coefficient. Figure 9 compares the experiment[36,39] with our calculation. There is a consistent difference between them: the experiment gives lower values of the ratio $R/(R+I)$ than the calculation. We now consider the origin of this discrepancy.

The first possibility is experimental: the apparent intensity of the intercombination line is enhanced by the mixing of impurity lines or satellite lines. We have looked for a possible impurity line that would contribute to the observed intensity of the intercombination (40.731 Å) line.[40] It is found that the line mixing is unlikely to occur. The satellite line intensity relative to the resonance-line intensity has been calculated by Gabriel *et al.*[41,42] using the corona equilibrium picture. Contribution may come from the satellites denoted as *m*, *n*, *s*, and *t*. Their total intensity is 0.1% of the resonance-line intensity, and if the plasma is ionizing the contribution should be almost the same. Thus, this possibility is ruled out. The next possibility is that some of the employed cross sections are wrong. Among them we first consider the ionization cross sections from the 2^3S and 2^3P levels: if they were decreased by a factor of 2 the calculated result would shift toward higher density by almost the same amount. The experimental data for $T_e>200$ eV would then become consistent with the calculation. However,

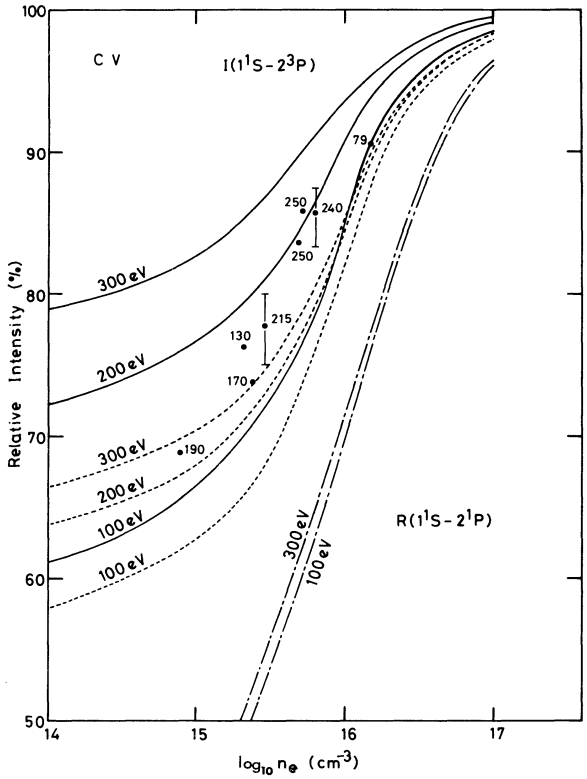

FIG. 9. Intensity ratio $R/(R+I)$ for C V. Solid lines show the results for the ionizing plasma, whereas the dotted lines and dashed-dotted lines indicate the results for the equilibrium plasma and the recombining plasma, respectively. Experiment is Ref. 39.

the error of a factor of 2 appears unlikely to occur in our ionization cross section and the lower-temperature data still remain inconsistent with the calculation. We thus rule out this possibility. Next is the excitation cross sections $1^1S\text{-}2^1P$ and $1^1S\text{-}2^3P$, by which the intensity ratio is largely determined. Our cross section for $1^1S\text{-}2^1P$ almost coincides with the distorted-wave polarized-orbital calculation by McDowell *et al.*[22] as for the case of oxygen, and this may be regarded as a lower bound for various existing calculations.[4] The cross section for $1^1S\text{-}2^3P$ almost coincides with the close-coupling calculation by Wyngaarden *et al.*[23]: this is just in-between of the existing larger and smaller cross sections. If we decrease $(1^1S\text{-}2^1P)$ by 20% or increase $(1^1S\text{-}2^3P)$ by the same amount, agreement within the experimental uncertainty would be obtained for the data for $T_e>200$ eV. This large modification to the cross sections, however, appears unrealistic and then a strong doubt would have to be cast on the scaling law of the cross section, since good agreement has been obtained for oxygen. Therefore, we abandon this possibility.

The next possible explanation is that the resonance line is not optically thin. However, under the experimental conditions the effect of radiation trapping should not affect the emission-line intensity of the resonance line as observed from the side of the theta-pinch plasma, or that as observed from the end and corrected for the radiation trapping effect.[39] This is because, for the 2^1P level, the

dominant depopulating mechanism is the radiative transition of the resonance line and the effective decrease in the transition probability due to the radiation trapping increases the upper-level population by the same amount. Thus the line intensity is not affected.

The last possibility is as follows: The assumption that the plasma condition is in the ionizing phase is not valid. In Fig. 9 also given are the intensity ratios calculated on the assumptions of the equilibrium plasma and the recombining plasma besides those for the ionizing plasma so far assumed. If we assume that the plasma is slightly ionizing and is close to equilibrium all of the data except for those for $T_e = 130$ and 79 eV are well interpreted. Our tentative conclusion is that the plasmas for the carbon experiment are somehow not predominantly ionizing, but they have appreciable contributions from the recombining plasma component.

V. CONCLUSIONS

We have completed the collisional-radiative program for heliumlike ions, and this has been applied to the interpretation of the experimental result of the line-intensity ratios that are obtained from the theta-pinch plasma. The data for oxygen have been successfully interpreted but those for carbon could not be fitted. A strong doubt has been raised about the nature of the latter plasma. In this kind of experiment it is extremely important to know in what plasma condition the plasma under study is, e.g., the predominantly ionizing, predominantly recombinating, or equilibrium plasma.

[1]T. Fujimoto, J. Phys. Soc. Jpn. **47**, 265 (1979); **47**, 273 (1979); **49**, 1561 (1980); **49**, 1569 (1980).

[2]D. R. Bates, A. E. Kingston, and R. W. P. McWhirter, Proc. R. Soc. **267**, 297 (1962); D. R. Bates and A. E. Kingston, Plant. Space Sci. **11**, 1 (1963); R. W. P. McWhirter and A. G. Hearn, Proc. Phys. Soc. **82**, 641 (1963).

[3]T. Fujimoto, J. Phys. Soc. Jpn. **34**, 216 (1973); **34**, 1429 (1973).

[4]T. Fujimoto and T. Kato, Astrophys. J. **246**, 994 (1981).

[5]T. Fujimoto, N. Yamaguchi, J. Mizui, T. Kato, and J. Fujita, J. Phys. D. **14**, 439 (1981).

[6]T. Fujimoto and T. Kato, Institute of Plasma Physics (Nagoya University) Report No. IPPJ-647 (1983) (unpublished).

[7]C. E. Moore, *Atomic Energy Levels,* Natl. Stand. Ref. Data Ser., Nat. Bur. Stand. (U.S.) Circ. No. 35 (U.S. GPO, Washington, D.C., 1971), Vol. I (H—V).

[8]S. Bashkin and J. O. Stone, Jr., *Atomic Energy Levels and Grotrian Diagram* (North-Holland, Amsterdam, New York, 1975), Vol. 1.

[9]R. M. Parish and R. W. Mires, Phys. Rev. A **4**, 2145 (1971); R. K. van den Eynde, G. Wiebes, and Th. Niemeyer, Physica **59**, 401 (1972).

[10]C. D. Lin, W. R. Johnson, and A. Dalgarno, Phys. Rev. A **15**, 154 (1977); Astrophys. J. **217**, 1001 (1977).

[11]S. A. Zapryagaev, V. G. Palchikov, and V. I. Safranova, Opt. and Spectrosc. **45**, 239 (1978).

[12]C. Laughlin, J. Phys. B **11**, L391 (1978).

[13]C. L. Cocke, B. Curnutte, and R. Randall, Phys. Rev. Lett. **31**, 507 (1973); S. L. Varghese, C. L. Cocke, and B. Curnutte, Phys. Rev. A **14**, 1792 (1976).

[14]W. A. Davis and R. Marrus, Phys. Rev. A **15**, 1963 (1977).

[15]W. J. Karzas and R. Latter, Astrophys. J. (Suppl.) **6**, 167 (1961).

[16]W. L. Wiese, M. W. Smith, and B. M. Glennon, *Atomic Transition Probabilities,* Natl. Stand. Ref. Data Ser., Nat. Bur. Stand. (U.S.) Circ. No. 4 (U.S. GPO, Washington, D. C., 1966), Vol. I.

[17]L. C. Green, N. C. Johnson, and E. K. Lolchin, Astrophys. J. **144**, 369 (1966).

[18]D. H. Sampson and A. D. Parks, Astrophys. J. (Suppl.) **28**, 323 (1974).

[19]A. K. Bhatia and A. Temkin, J. Phys. B **10**, 1829 (1977).

[20]D. Norcross, in *Electron Impact Excitation of Carbon and Oxygen Ions,* edited by M. H. Magee, Jr., J. B. Mann, A. L. Mertz, and W. D. Robb, [Los Alamos Scientific Laboratory Report No. LA-6691-MS (1977) (unpublished)].

[21]W. D. Robb, in *Electron Impact Excitation of Carbon and Oxygen Ions,* see Ref. 20.

[22]M. R. C. McDowell, L. A. Morgan, and T. Scott, J. Phys. B **10**, 2727 (1977).

[23]W. L. van Wyngaarden, K. Bhadra, and R. J. W. Henry, Phys. Rev. A **20**, 1409 (1979).

[24]A. K. Pradhan, D. W. Norcross, and D. G. Hummer, Phys. Rev. A **23**, 619 (1981).

[25]L. B. Golden and D. H. Sampson, J. Phys. B **10**, 2229 (1977).

[26]W. Lotz, Astrophys. J. (Suppl.) **15**, 307 (1971).

[27]Y. Itikawa and T. Kato, Institute of Plasma Physics (Nagoya University) Report No. IPPJ-AM-17 (1981) (unpublished).

[28]D. H. Crandall, R. A. Phaneuf, and D. C. Gregory, Oak Ridge National Laboratory Report No. ORNL/TM-7020 (1979) (unpublished).

[29]K. L. Bell and A. E. Kingston, J. Phys. B **4**, 1308 (1971).

[30]V. Jacobs, Phys. Rev. A **9**, 1938 (1974); Phys. Rev. Lett. **32**, 1399 (1974).

[31]F. B. Dunning and R. F. Stebbings, Phys. Rev. Lett. **32**, 1286 (1974).

[32]A. Burgess, Mem. R. Astron. Soc. **69**, 1 (1964).

[33]A. Burgess, D. G. Hummer, and J. A. Tully, Philos. Trans. R. Soc. London **A266**, 225 (1970).

[34]V. A. Boiko, A. Ya. Faenov, S. A. Pikuz, and U. I. Safranova, Mon. Not. R. Astron. Soc. **181**, 107 (1977).

[35]R. C. Elton and W. W. Köppendörfer, Phys. Rev. **160**, 194 (1967).

[36]H.-J. Kunze, A. H. Gabriel, and H. R. Griem, Phys. Rev. **165**, 267 (1968).

[37]A. Pospieszczyk, Astron. and Astrophys. **39**, 357 (1975).

[38]W. Engelhardt, W. Köppendörfer, and J. Sommer, Phys. Rev. A **6**, 1908 (1972).

[39]H.-J. Kunze, Phys. Rev. A **24**, 1096 (1981).

[40]R. L. Kelly, Oak Ridge National Laboratory Report No. 5922 (1982) (unpublished).

[41]A. H. Gabriel, Mon. Not. R. Astron. Soc. **160**, 99 (1972).

[42]C. D. Bhalla, A. H. Gabriel, and L. P. Presnyakov, Mon. Not. R. Astron. Soc. **172**, 359 (1975).